



## RESEARCH PAPER

# Single-nucleus RNA sequencing and mRNA hybridization indicate key bud events and *LcFT1* and *LcTFL1-2* mRNA transportability during floral transition in litchi

Ming-Chao Yang<sup>1, id</sup>, Zi-Chen Wu<sup>2, id</sup>, Ri-Yao Chen<sup>3</sup>, Farhat Abbas<sup>1, id</sup>, Gui-Bing Hu<sup>1, id</sup>, Xu-Ming Huang<sup>1, id</sup>, Wei-Song Guan<sup>1</sup>, Yi-Song Xu<sup>2</sup> and Hui-Cong Wang<sup>1,4,\* id</sup>

<sup>1</sup> Guangdong Laboratory for Lingnan Modern Agriculture/Key Laboratory of Biology and Genetic Improvement of Horticultural Crops-South China, College of Horticulture, South China Agricultural University, Guangzhou, China

<sup>2</sup> Becton Dickinson Medical Devices (Shanghai) Co., Ltd, Guangzhou, Guangdong, 510180, China

<sup>3</sup> College of Engineering, South China Agricultural University, Guangzhou, China

<sup>4</sup> Department of Life Sciences and Technology, Yangtze Normal University, Fuling 408100, China

\* Correspondence: [wanghc1972@263.net](mailto:wanghc1972@263.net)

Received 27 June 2022; Editorial decision 8 March 2023; Accepted 15 March 2023

Editor: Joanna Putterill, University of Auckland, New Zealand

## Abstract

In flowering plants, floral induction signals intersect at the shoot apex to modulate meristem determinacy and growth form. Here, we report a single-nucleus RNA sequence analysis of litchi apical buds at different developmental stages. A total of 41 641 nuclei expressing 21 402 genes were analyzed, revealing 35 cell clusters corresponding to 12 broad populations. We identify genes associated with floral transition and propose a model that profiles the key events associated with litchi floral meristem identity by analyzing 567 identified floral meristem cells at single cell resolution. Interestingly, single-nucleus RNA-sequencing data indicated that all putative *FT* and *TFL1* genes were not expressed in bud nuclei, but significant expression was detected in bud samples by RT-PCR. Based on the expression patterns and gene silencing results, we highlight the critical role of *LcTFL1-2* in inhibiting flowering and propose that the *LcFT1/LcTFL1-2* expression ratio may determine the success of floral transition. In addition, the transport of *LcFT1* and *LcTFL1-2* mRNA from the leaf to the shoot apical meristem is proposed based on *in situ* and dot-blot hybridization results. These findings allow a more comprehensive understanding of the molecular events during the litchi floral transition, as well as the identification of new regulators.

**Keywords:** Floral transition, *FLOWERING LOCUS T*, *Litchi chinensis*, mRNA transportation, single-nucleus transcriptome, *TERMINAL FLOWER 1*.

## Introduction

The switch from vegetative to reproductive growth, termed the floral transition, is a key event in the life cycle of angiosperms and is tightly linked to the annual yield of economically im-

portant crops. It involves flower bud differentiation, which has been divided into three independent phenological and developmental stages: floral induction, initiation, and development

(Meyerowitz *et al.*, 1991). The processes that define these stages are controlled by complex gene networks that respond to environmental and intrinsic signals, including nutritional state, day length, temperature, and the age of the plant (Andrés *et al.*, 2012; Bao *et al.*, 2020).

The vegetative shoot meristems of annual plants undergo floral transition to form determinate florescence meristems, and the plants die in the same growing season when all indeterminate meristems are lost. However, in perennial woody plants, some shoot meristems remain indeterminate to allow outgrowth in the following season, even when conditions permit sufficient flower induction at sexual maturity (Thomas *et al.*, 2000). The shoot meristem of woody plants is a highly dynamic structure, in which cells can rest or divide and the meristem can form vegetative shoots or inflorescences. Yet, a full understanding of the complex regulatory network of quiescent buds, buds transitioning from vegetative to reproductive growth, and breaking buds is still far from being achieved.

Floral initiation of many woody fruit crops is often erratic and varies considerably between varieties and in response to environmental conditions. Alternate- or biennial-bearing plants, which crop heavily in one year and then produce little or nothing the next, occur frequently in some fruit crop species, even under conditions that are favorable to flowering. As an example, litchi (*Litchi chinensis*), an economically significant evergreen fruit tree, has inconsistent flowering, and this issue is exacerbated by the changing climate and associated global warming (Menzel *et al.*, 2005). Chilling and shoot development patterns are fundamental for the success of litchi flowering (Ding *et al.*, 2015), and flowering can be induced only after a new shoot has been initiated, which means that an inductive signal acts only on actively growing buds (Menzel *et al.*, 2005). Notably, floral reversion, when a floral competent apical meristem fails to shift to reproductive growth and produce flowers, and instead remains vegetative and produces leaves, occurs frequently in litchi, especially in late-season cultivars. Taken together, these observations suggest that bud development plays a pivotal role in litchi flowering.

To investigate the molecular mechanisms that regulate floral transition, researchers have previously compared gene expression patterns in flowering and non-flowering buds (Zhang *et al.*, 2014; Chen *et al.*, 2018; Wang *et al.*, 2019). However, a bud is composed of multiple different cell types, whereas floral transition occurs only in a few cells. Consequently, critical differences in gene expression in key cells can be relatively very small compared with the entire bud transcriptome and thus overlooked. To address this limitation, in the current study three different bud types were sampled for single-nucleus RNA sequencing (snRNA-seq): undifferentiated buds (resting buds after 1 month of chilling induction), vegetative buds, and floral buds developed from undifferentiated buds. This allowed a high-resolution analysis of global gene expression profiles in a cell-type-specific manner and insights into molecular processes associated with bud rest, flower initiation, and differen-

tiation. These data will provide a valuable resource for future functional analysis of bud rest and flowering initiation and development in woody plants. Understanding the mechanism of floral induction in herbaceous plants, primarily *Arabidopsis* but also maize and rice, has been greatly advanced by using molecular and genetic tools. FLOWERING LOCUS T (FT) protein is transported to the shoot apex, where it interacts with the bZIP transcription factor FD (Turck *et al.*, 2008). At the shoot apex, the FT/FD complex binds to the promoter of *APETALA1* (*API*), which collaborates with the meristem identity gene *LEAFY* (*LFY*) to specify flower primordia at the shoot meristem flanks. Hsu *et al.* (2011) revealed that reproductive onset is determined by *FT1* in response to winter temperatures, whereas vegetative growth and inhibition of bud set are promoted by *FT2* in response to warm temperatures and long days in the growing season in the woody perennial poplar. The differential roles of *FT-like* genes, which modulate the annual growth cycle of poplar trees, was further confirmed through CRISPR/Cas9-mediated gene editing of individual gene members (André *et al.*, 2022). In aspen, FD-like 1 (FDL1) protein participates in the transcriptional control of the bud maturation pathway independent of its interaction with FT (Tylewicz *et al.*, 2015). These results suggest that the roles of the *FT* and *FD* genes might be more complicated in perennials than in annuals.

TERMINAL FLOWER 1 (TFL1), which is required to keep the inflorescence meristem in an indeterminate state, inhibits the expression of *LFY* and *API* in the inflorescence center (Yant *et al.*, 2009; Lee *et al.*, 2019). TFL1 interferes with the activity of FT or serves as a co-repressor, and the antagonism between TFL1 and FT depends on competition for shared target loci of FD (Zhu *et al.*, 2020). Although the central role of *FT* in the floral transition of the woody perennial litchi has been uncovered (Ding *et al.*, 2015), the molecular mechanism by which *FT* expression is regulated and the role of *TFL1* in flower transition remains uncertain. In this study, we use gene silencing, dot-blot, and *in situ* hybridization assays, as well as single-nucleus sequencing, to investigate and validate the role of *TFL1* in litchi flowering. We also provide evidence that *FT* and *TFL* mRNA are mobile signals transported from the leaf to the shoot apical meristem, which may play a critical role in litchi flowering.

## Materials and methods

### Plant material

Fifteen-year-old litchi trees (*Litchi chinensis* cv. ‘Guwei’) were selected as material for investigating the different regulatory mechanisms in buds in three developmental states at single-nucleus resolution. Chilling is essential for floral induction, although chilling requirements vary among litchi cultivars (Ding *et al.*, 2015). Generally, a shorter chilling period (about 1 month after bud rest) is sufficient for early-season cultivars to complete their floral induction, whereas late-season cultivars must experience a longer period of chilling (~2 months). ‘Guwei’ is a typical late-season litchi cultivar with high chilling requirements. The undetermined (U)

resting buds after 1 month of chilling induction, and the vegetative (V) and floral (F) buds that subsequently developed, were sampled. In addition, the leaves of cultivars '9911' (early-season), 'Feizixiao' (mid-season), 'Guwei' (late-season), and 'Nuomici' (late-season) were sampled from the resting bud stage to the floral initiation stage (the emergence of 'whitish millets') to monitor the expression of key floral induction genes. The litchi trees were grown in the experimental orchard of the South China Agricultural University and were maintained with standard horticultural practices.

#### Nuclei preparation for single-nucleus RNA sequencing

Terminal buds including shoot apical meristems and two axillary meristems along with rudimentary leaves were collected and immediately frozen in liquid nitrogen and stored at -80 °C until use. Approximately 20 buds were resuspended in 2 ml 10 mM MES nucleus isolation buffer (pH 5.7) containing 10 mM NaCl, 2.5 mM EDTA, 10 mM KCl, 250 mM sucrose, 1 mM DTT, 0.5% Triton X-100, 0.1% complete protease inhibitor cocktail (APExBIO), and 0.4 U  $\mu$ l<sup>-1</sup> RiboLock RNase inhibitor (Thermo Fisher Scientific, Cat. No. EO0382) and then homogenized on an MX-RL-E (DRAGONLAB). The homogenate was filtered through a cell strainer (40  $\mu$ m diameter) into a new tube and washed two or three times with nucleus isolation buffer. For sorting, the nuclei were stained with DAPI and loaded into a BD FACSMelody™ with a 100  $\mu$ m nozzle (Sunaga-Franze *et al.*, 2021). Approximately 120 000 nuclei were sorted based on the V450-A signal and the nuclear size. Cold Sample Buffer (2 ml, BD, Cat. No. 650000062) with 0.2 U  $\mu$ l<sup>-1</sup> RiboLock RNase inhibitor was used as a collection buffer. The quality of the nuclei was observed by using confocal microscopy (Zeiss LSM 800). The sorted nuclei were centrifuged (Eppendorf 5810R) at 1000 g at 4 °C for 5 min and Cold Sample Buffer was added to 1 ml. Detailed descriptions of the procedures can be found in Yang *et al.* (2022).

#### Single-nucleus capture and cDNA synthesis

Mass control of a single nucleus was based on the BD Rhapsody™ Scanner. The sorted nuclei were stained with 4  $\mu$ l DyeCycle Green (Thermo Fisher Scientific, Cat. No. V35004) for 5 min on ice and then loaded into a hemocytometer (INCYTO, Cat. No. DHC-N01-5). After counting single nuclei with the BD Rhapsody™ Scanner, a single-nucleus suspension was prepared for a BD Rhapsody cartridge (BD, Cat. No. 400000847) loading. Single-nucleus suspensions were determined, loaded into the cartridge, and incubated at room temperature for 30 min. Next, 630  $\mu$ l Cell Capture Beads (BD, Cat. No. 650000089) were loaded and washed, followed by lysis of the nuclei with 550  $\mu$ l Lysis Buffer (BD, Cat. No. 650000064) containing DTT and proteinase K (NEB, Cat. No. P81075). Finally, the cell capture beads were retrieved and washed. Reverse transcription was performed within 30 min using the BD Rhapsody™ cDNA Kit (BD, Cat. No. 633773) according to the manufacturer's instructions. After reverse transcription, beads were treated with 10  $\mu$ l Exonuclease I (BD, Cat. No. 650000072) and the bead suspension was incubated on a thermomixer at 1200 rpm at 37 °C for 30 min.

#### Whole-transcriptome analysis, library construction, and sequencing

The snRNA-seq libraries were constructed using the BD Rhapsody™ Cartridge Reagent Kit (BD, Cat. No. 633731) according to the instructions of the BD Single cell 3' whole-transcriptome amplification (WTA) kit. Briefly, Exonuclease I-treated beads in 1.5 ml tubes were treated to generate random priming and extension (RPE). The RPE product was then purified with AMPure XP beads followed by RPE PCR to generate more RPE product. Next, the RPE PCR amplification product was purified and measured using an Invitrogen Qubit™ 4 fluorometer and

an Agilent 2100 Bioanalyzer. After calculating the concentration of the purified product, WTA index PCR was performed to generate mRNA libraries compatible with the Illumina sequencing platform, by adding full-length Illumina sequencing adapters and indices through PCR. The concentration and qualitative analysis of the DNA library was performed by using the Invitrogen Qubit™ 4 fluorometer. After the quality of the libraries was checked, sequencing was performed using an Illumina NovaSeq 6000 (Novogene).

#### Single-nucleus RNA-sequencing data analysis and visualization

The raw data were analyzed using the Rhapsody WTA pipeline to obtain the cell-gene expression matrix file. The litchi genome and GTF annotation files were generated according to the Litchi Genome (Hu *et al.*, 2022). Reads were trimmed and quality-filtered using the Rhapsody WTA pipeline and aligned using STAR v.2.5.2b (Dobin *et al.*, 2013). The cell-gene expression matrix files were used for data analysis and visualization with the SeqGeq™ Software v1.7 (FlowJo LLC, Ashland, CA, USA).

#### Virus-induced gene silencing-mediated silencing of gene expression

Virus-induced gene silencing (VIGS) was carried out as previously described (Wu *et al.*, 2018). Fragments of *LcTFL1-2* (437 bp) were inserted into the TRV2 vector to generate pTRV2-*LcTFL1-2*. Shoot injection was employed for silencing of the gene, with a bacterial concentration of OD<sub>600</sub>≈1.0. The bacterial suspension was injected into the middle stem of a resting autumn shoot ~1 month before floral initiation. Thirty shoots located in different parts of each of the three 'Nuomici' canopies were treated. Among these 20 shoots were used to investigate the flowering rate and the remaining 10 shoots were used for sampling. Leaf and bud samples were collected 3 weeks after injection to test the silencing effects and to perform RNA-seq analysis. The specific primer pairs used are listed in Supplementary Table S1.

#### RNA extraction and quantitative RT-PCR analysis

Total RNA was isolated from the samples using a Quick RNA isolation Kit (Huayueyang Biotech, Beijing, China). First-strand cDNA synthesis was performed using 2  $\mu$ g total RNA with the RevertAid First strand cDNA Synthesis Kit, according to the manufacturer's instructions (Thermo Fisher Scientific, Cat. No. 00994100). *LcFT1* and *LcTFL1-2* transcript levels were determined by quantitative reverse transcription-PCR (qRT-PCR) analysis according to Lai *et al.* (2015). Each sample was quantified in four biological replicates and normalized to the Cp values of the *LcActin* (HQ615689.1) and *LcGAPDH* (JF759907.2) house-keeping genes. The gene-specific primer pairs are listed in Supplementary Table S1.

#### RNA *in situ* and dot-blot hybridization

Specific sequences of *LcFT1* and *LcTFL1-2* cDNA (181 bp and 191 bp, respectively) were cloned into the pGEM-T easy vector (Promega, Fitchburg, WI, USA). *In vitro* synthesis and labeling of RNA probes was performed using a DIG RNA Labeling Kit (SP6/T7) (Roche, Basel, Switzerland). The labeling efficiency of the probes was detected using a DIG Nucleic Acid Detection Kit (Roche) according to the DIG Application Manual for Nonradioactive *In Situ* Hybridization (Roche). RNA *in situ* hybridization was performed as described by Lou *et al.* (2017). Images were obtained using an Axio Imager DPTOP CX40 microscope (Zeiss).

For dot-blot hybridization, total RNA was isolated from buds, leaves, and stems using a Quick RNA isolation Kit (Huayueyang Biotech, Beijing, China). The mRNA was purified by using the PolyAtract®

mRNA Isolation System IV (Promega). Samples of ~100 mg were used for nuclei isolation and nuclei were sorted by flow cytometry (BD FAC-SMelody<sup>TM</sup>). The nuclear RNA was isolated. The dot-blot assay was performed as described by Green *et al.* (2022).

## Results

### *Developmental pattern and morphology of litchi buds*

In litchi, periods of stem elongation are separated by periods of stasis, when the terminal bud is at rest (quiescent) or a terminal inflorescence has formed. A terminal resting bud contains apical and axillary meristems and rudimentary leaves (Fig. 1A). The axillary or apical meristem may transition from the undifferentiated state to the panicle-competent state in response to prolonged chilling. At this stage, morphological changes are not yet visible, but induction takes place. Subsequently, the buds may break and elongate when the atmospheric temperature rises. The inflorescence-competent meristem develops into floral primordia, which are visible to the naked eye and are named ‘whitish millets’ for their white color, which results from a high density of trichomes. In some cases, a winter resting bud can develop into a vegetative shoot due to failed floral induction or initiation.

### *Single-nucleus sequencing of litchi buds*

Litchi is a highly waxy woody plant, and it can be technically difficult to isolate pure protoplasts. Indeed, the protoplast samples generated in our studies contained cell wall debris,

ruptured protoplasts, and cells from which the cell wall had not been digested (Supplementary Fig. S1A) and so did not meet the quality requirements for single-cell sequencing. As an alternative strategy, we used single-nucleus sequencing to investigate the transcriptome of individual cells (Bakken *et al.*, 2018; Wu *et al.*, 2019), and established a method to isolate high-quality nuclei from litchi buds for snRNA-seq analysis.

When we initially isolated nuclei from the buds, substantial amounts of cellular debris were present in the samples, even after washing with isolation buffer. To purify the samples further, we collected nuclei using flow cytometry based on nuclear size and staining with DAPI (Fig. 1B). Observation of the sorted nuclei with a confocal laser scanning microscope indicated that the samples were of high quality, and the nuclei were then loaded into a BD Rhapsody<sup>TM</sup> cartridge for single-nucleus RNA-seq (Supplementary Fig. S1B).

After establishing the high-purity nucleus-separation system, we constructed a WTA library using the BD Rhapsody<sup>TM</sup> platform and sequenced the samples on an Illumina NovaSeq sequencer. The detailed procedure is shown in Supplementary Fig. S2. The transcriptomes of three bud samples were annotated according to the litchi genome and cell–gene expression matrices were created separately. Three matrices were then concatenated into one matrix using the SeqGeq platform. After quality control and filtration to eliminate multiple cells and cells with very low gene expression, 41 641 high-quality nuclei

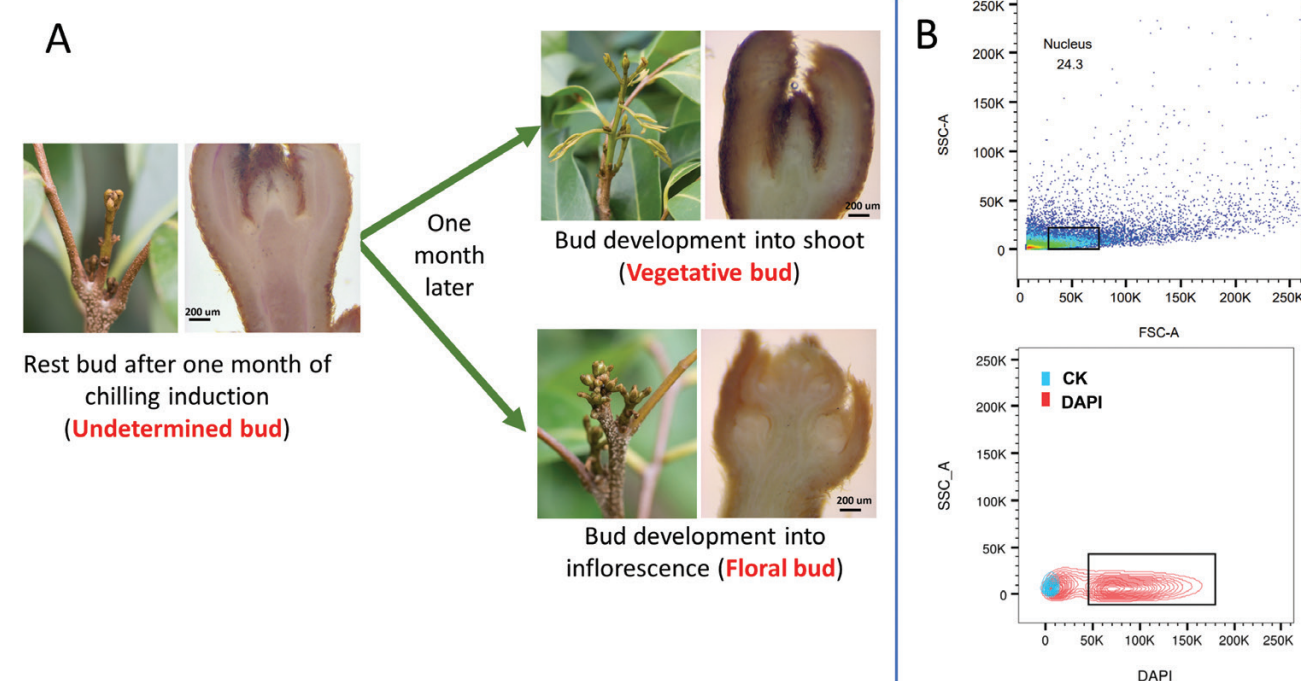


**Fig. 1.** Images of litchi bud samples and the quality control of the isolated bud nuclei. (A) Macroscopic and microscopic images of buds from three different developmental stages. (B) Nucleus quality control using flow cytometry.

were obtained (Supplementary Fig. S3) and the expression of 21 402 genes was detected, with approximately 12 000–16 000 nuclei per sample and 394–872 unique gene expression signals per nucleus.

#### Generation of a *litchi* apical bud cell atlas

BatchLR analyses were run with the 41 641 high-quality nuclei and the highly dispersed genes between the three bud samples and then a t-distribution stochastic neighborhood embedding (t-SNE) tool was used to analyze the datasets (Haghverdi *et al.*, 2018; Belkina *et al.*, 2019) (Fig. 2A). A K-means-based clustering analysis revealed 20 distinct cell clusters (Fig. 2B); by comparing the cell atlas between the three bud types, we found that the cell atlas of the floral bud was distinct from that of the other two samples (Supplementary Fig. S4). We then characterized specific cell populations in the three samples according to the expression patterns of each cluster (Fig. 2C, D; Supplementary Fig. S4A). Twenty clusters could clearly be

characterized as five predominant populations: undetermined (U), floral (F), vegetative (V), vegetative plus undetermined (V+U), and vegetative plus floral (V+F). The cell numbers of the different cell populations ranged from 2742 to 11703 (Supplementary Fig. S4B).

A K-means-based clustering method was applied to a regenerated cell atlas of U, V, and F cell populations, and 35 distinct cell clusters were observed (Fig. 3A). A heatmap was used to show the expression pattern of 13 marker genes among the 35 detected clusters, and the clusters were then defined and annotated according to characteristically expressed marker genes with distinct molecular functions (Fig. 3B). The mesophyll cell (MC) population consisted of seven clusters (clusters A1, A3, A10, A21, A24, A27 and A34) in which genes involved in photosynthesis, such as *RUBISCO BISPOSPHATE CARBOXYLASE SMALL SUBUNIT 1* (*RBCS1*) (Pichersky *et al.*, 1986), *LIPOXYGENASE 2.1* (*LOX2.1*), and *LOX6* (Jensen *et al.*, 2002; Neumann *et al.*, 2021), were predominantly expressed. The epidermis cell (EC) population was composed

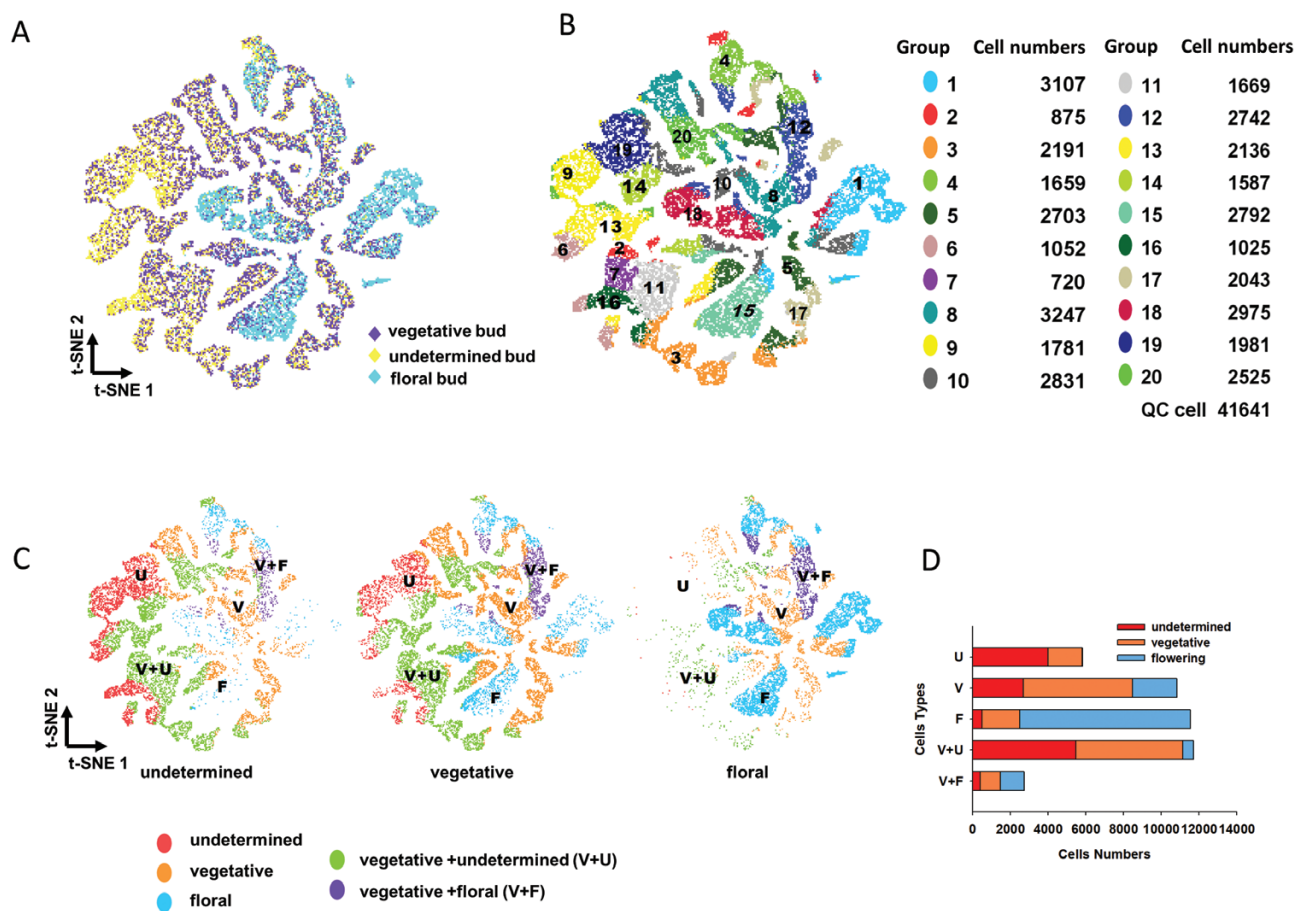


**Fig. 2.** Generation of *litchi* bud radicle cell atlases. (A) t-SNE visualization of cells from undetermined (U, yellow;  $n=13\,082$ ), vegetative (V, purple;  $n=16\,341$ ), and flowering (F, blue;  $n=12\,218$ ) buds. Dots represent individual cells and colors represent different bud types. (B) t-SNE visualization identifying 20 putative cell clusters from 41 641 bud cells. Each dot denotes a single cell. Colors denote corresponding cell clusters. (C) t-SNE visualization identifying dominant cell clusters among the three bud types. Colors denote different dominant cell clusters. (D) Cell numbers in the dominant clusters among the three bud types.

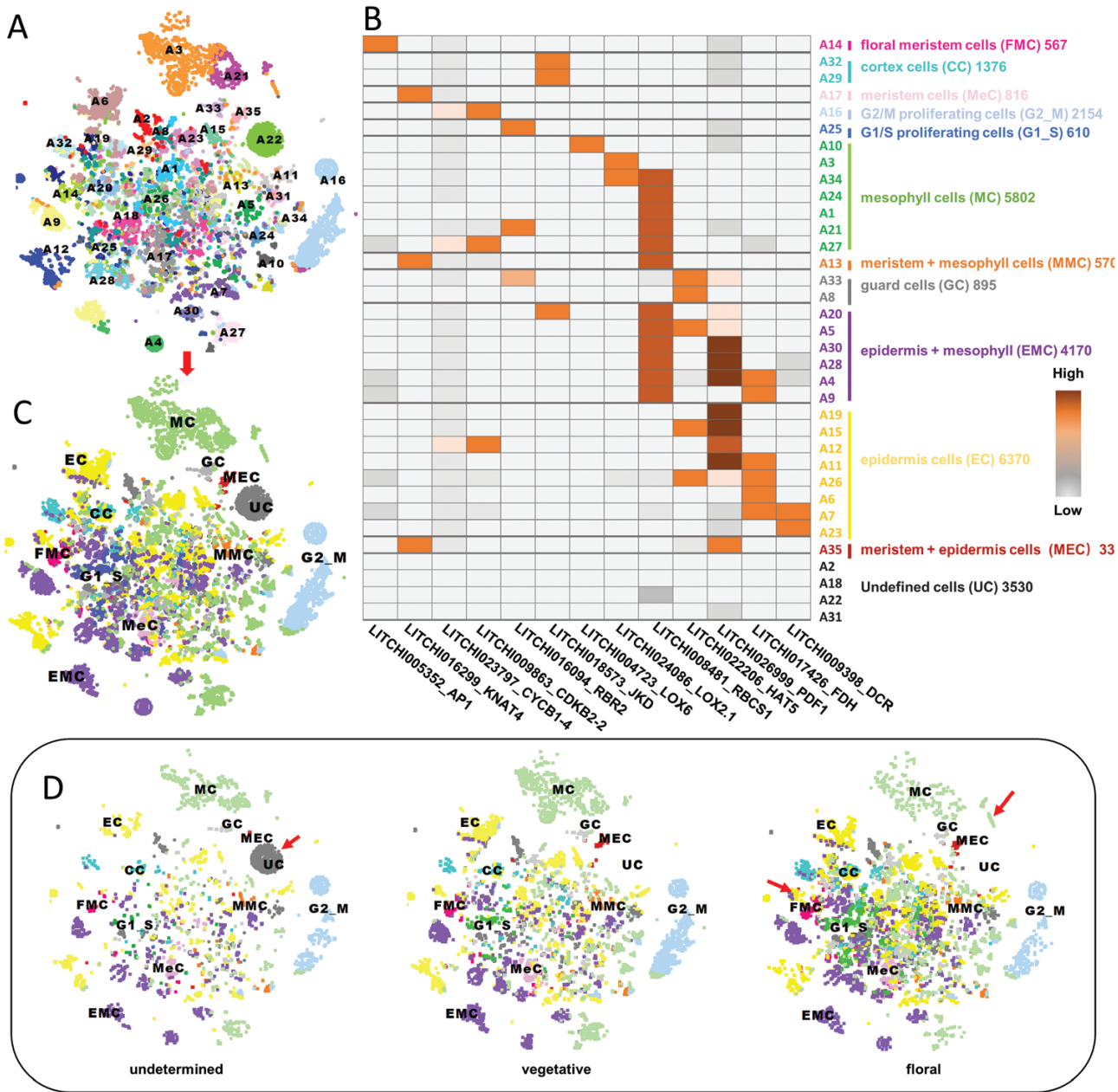


**Fig. 3.** Heterogeneity analysis of cells in different litchi bud types. (A) t-SNE visualization identifying 35 putative cell clusters from 27 196 different cells. Each dot denotes a single cell. Colors denote corresponding cell clusters. (B) Expression patterns of representative cluster-specific marker genes. AP1, APETALA1; KNAT4, HOMEBOX PROTEIN KNOTTED-1-LIKE 4; CYCB1-4, CYCLIN B 1-4; CDKB2-2, CYCLIN-dependent kinase B 2-2; RBR2, RETINOBLASTOMA-RELATED PROTEIN 2; JKD, JACKDAW; LOX2.1, LIPOXYGENASE 2.1; RBCS1, RUBISCO BISPOSPHATE CARBOXYLASE SMALL SUBUNIT 1; HAT5, HOMEBOX-LEUCINE ZIPPER PROTEIN HAT5; PDF1, PROTODERMAL FACTOR 1; FDH, FIDDLEHEAD; DCR, DEFECTIVE IN CUTICULAR RIDGES. (C) t-SNE visualization of 12 populations. Colors represent population types. (D) t-SNE plot showing 12 cell populations from the three bud types. Each dot denotes a single cell. Colors denote corresponding cell clusters. Red arrows indicate the differentially expressing cells.

of eight clusters (A6, A7, A11, A12, A13, A15, A19, and A26) and included the epidermal-specific genes *PROTODERMAL FACTOR1* (PDF1), *FIDDLEHEAD* (FDH) (Abe et al., 2003), and *DEFECTIVE IN CUTICULAR RIDGES* (DCR) (Zhang et al., 2021b). Cluster A17 was distinct for meristem cells (MeC), since it specifically expressed *HOMEBOX PROTEIN KNOTTED-1-LIKE 4* (KNAT4) (Zhang et al., 2021b).

The floral meristem cell (FMC) population consisted of cluster A14, in which *AP1* (Neumann et al., 2021) was expressed. Additionally, G1/S proliferating, G2/M proliferating, cortex cells (CC), guard cells (GC), meristem plus mesophyll cells (MMC; expressing both the *KNAT4* and *RBCS1* genes), epidermis plus mesophyll cells (EMC), and meristem plus epidermal cells (MEC) populations were defined (Lopez-Anido et al., 2021).

Clusters A2, A18, A22, and A31 were not defined (undefined cells; UC) because no corresponding characteristic marker gene was identified. Each cell population contained between 336 and 6370 single cells (Supplementary Fig. S4C). Finally, a t-SNE visualization of 12 defined cell populations was created (Fig. 3C).

To investigate the differences in cell populations among the bud types, t-SNE visualization of 12 defined cell populations from each bud type was generated. Comparing the cell atlases from the three bud types, two specific cell populations were observed (Fig. 3D): one group of undefined cells was specifically present in U buds, and some cells defined as mesophyll cells were found only in F buds.

#### Comparison of different bud types at single-cell resolution

To identify key genes associated with bud rest and floral transition, we further analyzed the abovementioned undefined cells in U buds and floral bud-specific mesophyll cells and the FMC population (Fig. 4). The gene expression in cells found only in floral buds ('F\_only') was compared with that of the remaining cells ('F\_only-') (Fig. 4A). In this way, we were able to identify differences in transcript abundance in these populations. The 113 'F\_only' cells showed specific expression of a putative litchi *AP1* (*LcAP1*, LITCHI005352) in addition to the mesophyll marker gene *LOX2.1* (LITCHI024086). However, genes involved in photosynthesis (*RBCS1*, LITCHI008481), epidermal cell differentiation as well as fatty acid metabolism and elongation (*FDH*, LITCHI017426), and leaf development (*PDF1*, LITCHI026999) were not expressed (Fig. 4B, C). These cells represent the primordia of floral organs or tissues, since *LOX2.1* has also been reported to be active in stamens and sepals (Rubio-Somoza and Weigel, 2013; Neumann *et al.*, 2021).

Cells found only in the U category ('U\_only') had low, or even no, expression of hundreds of genes, with fewer higher-expression genes (Fig. 4D). Gene Ontology (GO) analysis of genes with lower transcript abundance in 'U\_only' cells showed enrichment of annotation terms involving transportation (Fig. 4E), which indicated that this cell population was relatively isolated. Interestingly, among the genes with higher expression, an uncharacterized gene (LITCHI014472) was observed to be specifically expressed in 'U\_only' cells (Fig. 4F). This gene might be a target for further studies of bud development and floral transition.

A total of 567 cells were defined as FMC, but the number of FMC cells varied among bud types. The cell number was much lower for the U bud category (34 cells) than in the V bud (209 cells) and F bud (324 cells) categories (Fig. 4A). To compare the expression profiles of floral-related genes in FMC among the three bud types, we reduced the cell number to 34 through random cell selection in the V and F bud samples in SeqGeq and made a cell-gene histogram (Fig. 4G). Putative *AP1* (LITCHI005352), *AGAMOUS-like*

*MADS-box protein 8* (*AGL8*, LITCHI023327), and *LEAFY* (LITCHI020239) were dominantly expressed in FMCs of F buds. The number of cells expressing a putative DELLA protein gene (*GAI*, LITCHI008177) was largest in F bud samples, followed by V and U buds. Intriguingly, putative *SUPPRESSOR OF CONSTANS OVEREXPRESSION 1* (*SOC1*, LITCHI025598) and a bZIP transcription factor (*FD*, LITCHI006416), which have been reported to combine with *FT* to activate floral identity genes such as *AP1* (Wigge *et al.*, 2005; Tylewicz *et al.*, 2015), had lower expression in F buds. Putative *SQUAMOSA PROMOTER-BINDING-LIKE PROTEIN 8* (*SPL8*, LITCHI025415), *FLOWERING LOCUS C* (*FLC*, LITCHI004635), and the floral homeotic protein gene *APETALA 2* (*AP2*, LITCHI006915) were highly expressed in V buds but expressed at low levels in F buds.

Floral transition depends on a complex regulatory network. To determine the regulatory network underlying the 567 FMCs, we next analyzed expression correlations between a set of flowering-related genes that had previously been identified *in planta* at single-cell resolution (Fig. 5). In the FMC population, we identified a putative *HOS1* (LITCHI022757), a gene that controls flowering time in response to ambient temperatures and that negatively regulates CONSTANS abundance in the photoperiodic control of flowering in *Arabidopsis thaliana* (Lazaro *et al.*, 2012; Lee *et al.*, 2012). We also found a putative *GAI* (LITCHI008177), which may serve as a major and highly connected central regulator, as well as putative *AP1* (LITCHI005352), *AGL8* (LITCHI023327), *AP2* (LITCHI018533), *RAP2-4* (LITCHI010452), *CRY1* (LITCHI010518), and *LEAFY* (LITCHI020239). Intriguingly, the expression of the abovementioned putative *GAI* and *AP2* showed a predominantly negative correlation with the other components of the network. The expression of the putative *HOS1* (LITCHI022757) showed a strong positive correlation with the expression of putative *AGL8* (LITCHI023327) and *SHORT VEGETATIVE PHASE* (*SVP*, LITCHI001246), but was negatively related to putative *LEAFY*, *CRY1* (LITCHI010518), *AGL42* (LITCHI009244), and *SVP* (LITCHI007230) expression. The expression of putative litchi *AP1*, a gene that functions mainly as an activator in other plants (Yant *et al.*, 2009), was strongly positively correlated with the expression of putative *AGL8* (LITCHI023327), *FD* (LITCHI006416), *AGL62* (LITCHI008609) and *SPL8* (LITCHI025415). *AGL42* has been reported to promote flowering at shoot apical and axillary meristems in *A. thaliana* (Dorca-Fornell *et al.*, 2011). In the current study, the expression of a putative *AGL42* (LITCHI009244) was highly correlated with that of a putative *LEAFY* (LITCHI020239) gene.

#### Reconstruction of the differentiation trajectory of bud cells from a single-cell snapshot

As we investigated buds from three different developmental stages and they showed significant differences in gene

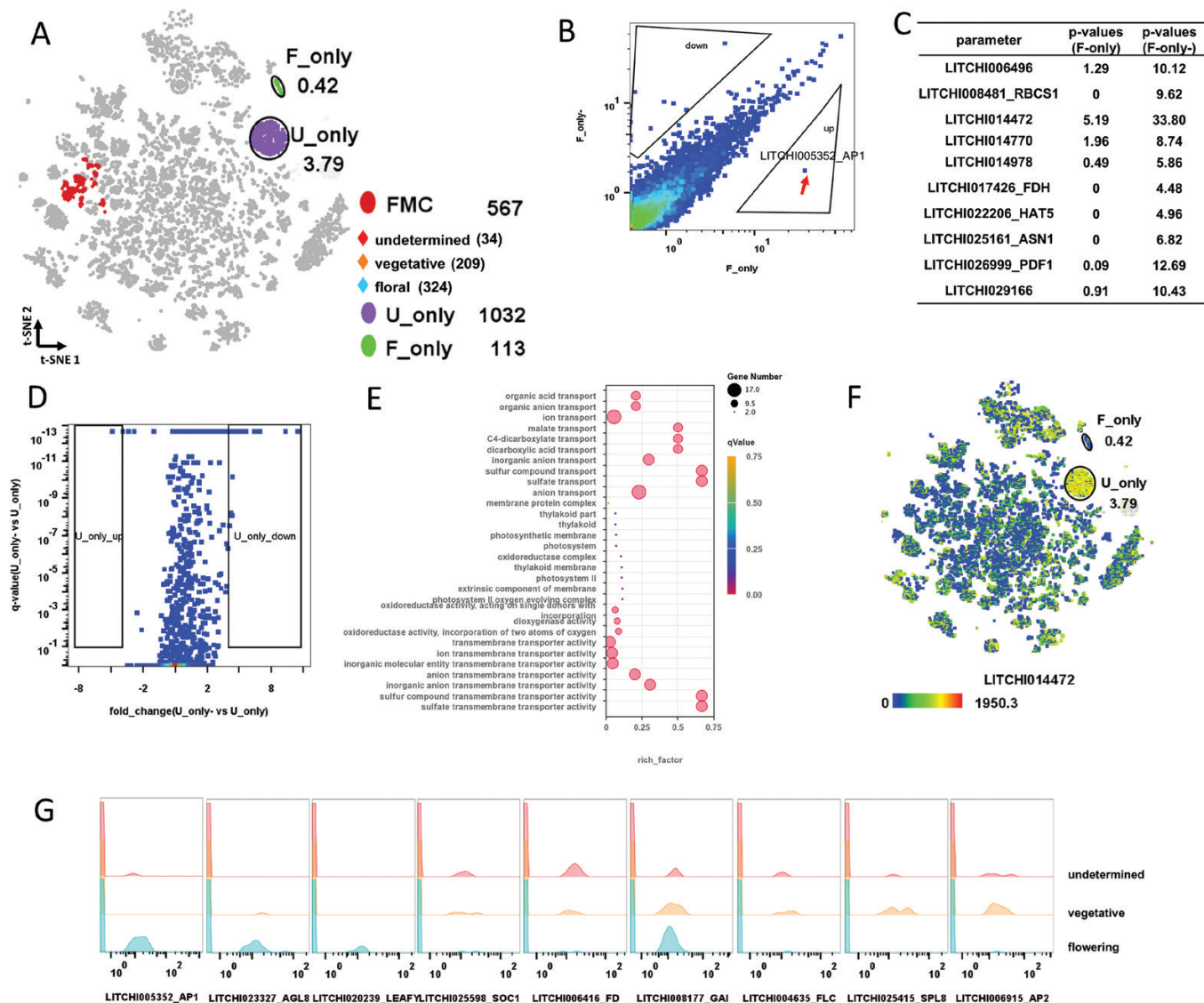


**Fig. 4.** Comparison of different cell populations at single-cell resolution. (A) t-SNE visualization showing three specific cell populations and their cell numbers. (B) Gene expression pattern in 113 floral bud-specific mesophyll cluster cells compared with resting cells. Each dot denotes a single gene. (C) Down-regulated genes in the 113 'F\_only' cells. (D, E) Gene expression pattern (D) and Gene Ontology analysis (E) of down-regulated genes in the 1032 undefined cells. (F) t-SNE plot showing one specific highly expressed gene in the 1032 undefined cells. (G) Histogram showing cell numbers and expression levels of key floral genes in the floral meristem cells of the three bud types.

expression patterns, the snRNA-seq data enabled an analysis of the differentiation trajectory during bud development. To this end, we used 943 highly variably expressed genes to visualize the closest possible equivalent fuzzy topological structure among cells from the U,V, and F populations (Fig. 6A). We employed Monocle, an algorithm that uses graph embedding to describe multiple fate decisions (Trapnell *et al.*, 2014), to reveal the hierarchical structures of the cells from the three bud types (Fig. 6B). The cells were divided into four different subsets, which we named direction 1 to direction 4 (d1–d4). The U bud cells were found to mainly assemble at the end of d1 and d2. D3 could be attributed to F buds, while d4 was associated

with V buds. In the center region (cr) that connected the four subsets, cells from all three bud types were present.

Cells from U buds (d1 and d2) showed high expression of a putative gene involved in gluconeogenesis, phosphoenolpyruvate carboxykinase (*PCKA*, LITCHI007159), a gene connected to regulation of the circadian rhythm, cryptochrome-2 (*CRY2*, LITCHI015320), and an ethylene-responsive element, *RAP2-3* (LITCHI014444), which may be involved in the regulation of gene expression by stress factors and by components of stress signal transduction pathways (Buttner *et al.*, 1997) (Supplementary Fig. S5A). The roles of these genes in retaining the bud resting state remains to be elucidated.

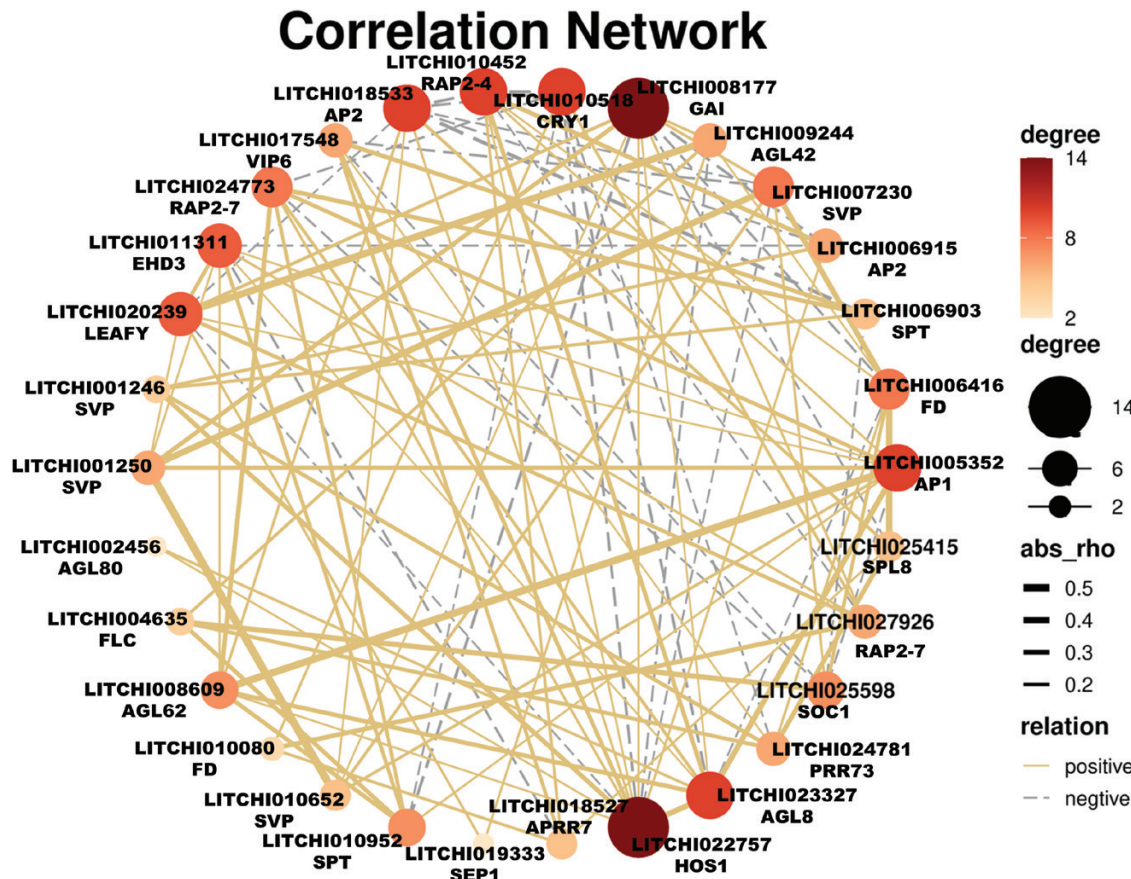


**Fig. 5.** Correlation of expression among flowering-related genes in the 567 floral meristem cells at single-cell resolution. AGL, AGAMOUS-like MADS-box; AP1, APETALA1; AP2, APETALA2; APRR, ARABIDOPSIS PSEUDO RESPONSE REGULATOR; FD, FLOWERING LOCUS D; FLC, FLOWERING LOCUS C; CRY1, CRYPTOCHROME 1; EHD, EARLY HEADING DATE; HOS1, E3 UBIQUITIN LIGASE HIGH EXPRESSION OF OSMOTICALLY RESPONSIVE GENE 1; GAI, GIBBERELLIC ACID INSENSITIVE; LFY, LEAFY; PRR73, PSEUDO RESPONSE REGULATOR 73; RAP2-4, ETHYLENE-RESPONSIVE TF RAP2-4; SEP, SEPALLATA; SPL, SQUAMOSA-PROMOTER BINDING PROTEIN-LIKE; SPT, SPATULA; SOC1, SUPPRESSOR OF EXPRESSION OF CO 1; SVP, SHORT VEGETATIVE PHASE; VIP, VERNALIZATION INDEPENDENCE.

A putative floral suppressor *FLC* (LITCHI004635), *SVP* (LITCHI010652, LITCHI001247, LITCHI001249, LITCHI001251), a putative *SPL8* (LITCHI025415), a downstream regulator in the ethylene signaling pathway related to *APETALA2* 2 (*RAP2-2*, LITCHI029903), *MADS-box transcription factor 21* (*MADS21*, LITCHI004591), and a zinc finger protein, *CONSTANS Like 15* (*COL15*, LITCHI004591), were expressed at much lower levels in the cells attributed to F buds (d3) than in those of the other directions (Supplementary Figs S4D, S5B).

*AP1* and *AGL8*, a homolog of the MADS-box gene *FRUITFULL* (*FUL*), act redundantly in their control of inflorescence architecture, which involves modulating *LFY* and *TFL1* expression as well as the relative level of their activities (Ferrandiz *et al.*, 2000). The putative litchi *AP1*, *AGL8*, and *EARLY FLOWERING 3-2* (*ELF3-2*, LITCHI007019), which encodes a protein required for photoperiodic flowering (Hicks *et al.*, 2001), were prominently expressed in the F bud cells (Supplementary Fig. S5C). Another two less-studied

MADS-box genes, *ENHANCER OF JOINTLESS 2* (*EJ2*, LITCHI005351 and LITCHI023328), were also found to be mainly expressed in F bud cells (d3).

*FT*, *TFL*, *FD*, *SOC1*, *LEAFY*, *GAI*, and *AP2* are key genes in the flowering pathway (Yant *et al.*, 2009). No putative *FT* (LITCHI002331) or *TFL1* (LITCHI024460) gene was detected in the nuclear transcriptome data of the cells of any of the four directions (Supplementary Fig. S5D). However, as we had identified four *FT* and two *TFL1* homologs in the litchi genome, we sought to confirm the absence of nuclear expression by investigating their expression patterns in the different cell populations of buds, together with other floral-related genes that were previously found to be differentially expressed among FMCs of different bud types as references (Supplementary Fig. S6). As shown in the histogram of the cell number and transcription levels of 12 floral-related genes, no single cell expressed the putative litchi *FT* and *TFL1* (Supplementary Fig. S6B). The expression of putative *FD* (LITCHI006416) was much lower in the F cells than in the U and V cells, and

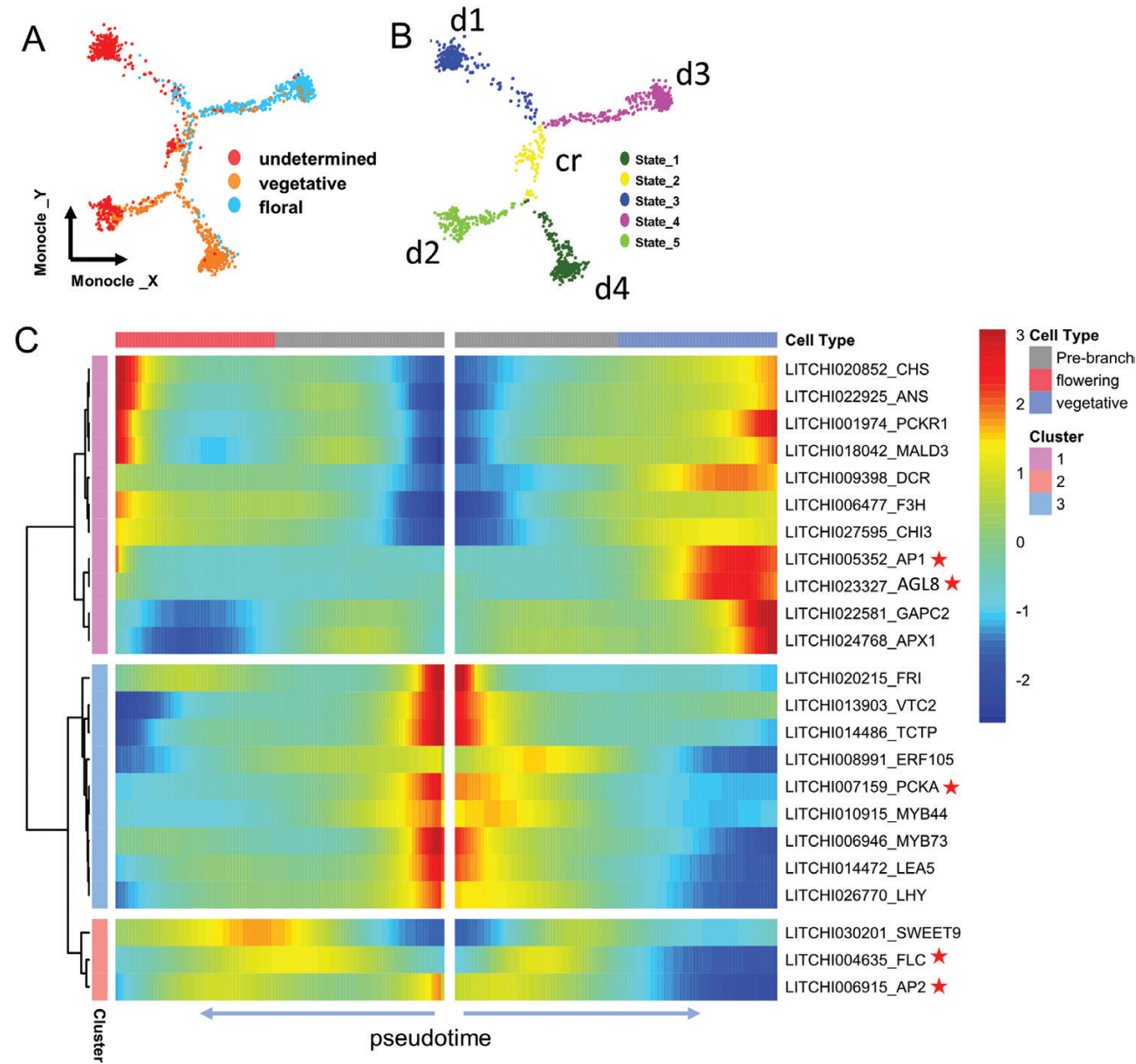


**Fig. 6.** Bud differentiation trajectories. (A) Simulation of the differentiation trajectory of bud cells in pseudo-time. Cells from undetermined, vegetative, or floral buds are shown over the course of pseudo-time. Dots, individual cells; color, bud types. (B) Re-definition of the cells according to their differentiation direction. Dots represent individual cells; different colors indicate different bud types. d, direction; cr, center region. (C) Heatmap of the genes that are associated with the pseudo-time progression of floral or vegetative growth. Three distinct gene clusters were identified, each with a different activity region during the developmental process. Red stars indicate important flowering-related genes.

putative *LEAFY*, *GAI*, and *AP2* (*LITCHI006915*) were found to be constitutively expressed in all the cells (Supplementary Fig. S6).

A pseudo-time branch heatmap with three distinct clusters of genes related to vegetative or floral growth was generated (Fig. 6C). *AP1*, *AGL8*, *AP2*, *FLC*, and *PCKA* were found in three different clusters, each of which was in a different activity region during the developmental process (Fig. 6C). The

pseudo-time heatmap reflects the flowering or vegetative trajectory process well.

#### The role of LcTFL1-2 in floral transition and mRNA transport of FT and TFL1

FT functions as a mobile florigen that travels from the leaf to the shoot meristem to trigger flowering (Turnbull, 2011). In

litchi, *LcFT1* (LITCHI002331) has been identified as a floral integrator gene: its overexpression in tobacco and Arabidopsis plants induced precocious flowering (Ding *et al.*, 2015). *TFL1* is another gene that functions as an important regulator of flowering time, and its overexpression results in late flowering (Benloch *et al.*, 2007). However, no *FT1* or *TFL1* was detected in the 43 750 nuclei tested according to our snRNA-seq dataset (PRJNA909160). This result has drawn our particular attention because noticeable expression of *LcFT1* and *LcTFL1-2* was previously observed in bud tissue of litchi.

*LcFT1* and *LcTFL1-2* (LITCHI024460) are the predominantly expressed *FT/TFL* members in litchi leaves. In the present study, four cultivars differing in flowering time were selected to investigate the expression of *LcFT1* and *LcTFL1-2* during floral transition. Although the relative expression levels showed marked differences among the four cultivars, the transcription of *LcFT1* increased in all four immediately prior to floral initiation (Fig. 7A). The early-flowering litchi cultivar 9911 displayed the lowest *LcFT1* expression at floral initiation, suggesting that an increase in expression is essential for the floral transition but the absolute expression level differs among cultivars. We also examined *LcTFL1-2* expression in the leaves of the four cultivars during floral transition and found that the expression levels in the early- and mid-season cultivars 9911 and Feizixiao were much lower than those in the late-season cultivars Nuomici and Geiwei (Fig. 7A). This result was consistent with studies in other plants suggesting that *TFL1-2* may serve as an inhibitor of floral transition in litchi. To confirm the role of *LcTFL1-2* in litchi floral transition, we silenced its expression using VIGS. Compared with negative control plants harboring a pTRV2 empty vector, the expression of *LcTFL1-2* was significantly reduced in both the silenced bud and leaf samples (Fig. 7B). We observed a significant increase in flowering rate in response to *LcTFL1-2* down-regulation, suggesting that *LcTFL1-2* acts as a floral inhibitor (Fig. 7C).

As mentioned earlier, no transcription of putative litchi *FT* and *TFL1* was detected in the snRNA-seq data of the three bud types, but using qRT-PCR detection, we detected the expression of *LcFT1* and *LcTFL1-2* in bud and leaf samples. We then extracted the nuclei from buds and measured the expression levels of these genes by using qRT-PCR, and compared them with expression levels of the same genes in intact buds, and intact leaf samples, and leaf nuclei. Consistent with the snRNA-seq result, no *LcFT1* and *LcTFL1-2* transcription was detected in bud nuclei, whereas expression of both genes was observed in intact buds, leaf nuclei, and intact leaf samples (Fig. 7D).

To confirm the presence of *FT* and *TFL1* mRNA in litchi buds, we used mRNA *in situ* and dot-blot hybridization assays. *LcFT1* and *LcTFL1-2* mRNA was detected in leaf vasculature and phloem cells, and was also clearly observed in meristem cells of both floral and vegetative buds, with floral buds having

higher *LcFT1* mRNA levels than vegetative buds (Fig. 8A). FT protein is a mobile signal that travels from the leaf to the shoot apical meristem to cause changes in gene expression that reprogram the plant to form flowers or inflorescence (Turck *et al.*, 2008). The *LcFT1* and *LcTFL1-2* mRNA detected in meristem cells could be produced *in situ* or transported from the leaf. To confirm that the detected bud *LcFT1* and *LcTFL1-2* were not the result of *in situ* transcription, we detected their presence in total RNA, mRNA, and nuclear RNA extracted from floral bud, vegetative bud, leaf, and stem samples. *LcFT1* and *LcTFL1-2* mRNA was detected in all samples of total RNA and mRNA, but in nuclear RNA only from leaf samples (Fig. 8B).

## Discussion

### The generation of a litchi shoot apex cell atlas

The floral transition in woody litchi is a complex process involving four major phases (Menzel *et al.*, 2005). The first involves growth cessation, bud set, and bud rest, which are prerequisites for floral transition. Second, and probably consistent with the role of a systemic floral regulator or florigen in the flowering of herbaceous plants such as Arabidopsis, rice, and tomato (Putterill *et al.*, 2016), *FT* or *FT* analogues are synthesized in the leaf in response to a prolonged chilling stimulus. Third, after floral induction, the onset of shoot development is essential for a meristem to develop into a floral primordium in response to flowering signals (floral initiation). Finally, successful development of inflorescence is also critical. Even though the physiological and phenotypic changes of the apical bud are central to the successful development of inflorescences in litchi, no study of these events has been reported to date.

Recently, the application of single-cell (sc)RNA-seq has been described for functional studies and gene discovery in *A. thaliana* and *Oryza sativa* (Zhang *et al.*, 2019, 2021a). Since it is particularly difficult to isolate protoplasts from the tissues of perennial woody plants because of their rigid secondary cell walls, single-nuclei (sn)RNA-seq represents a promising alternative for surveying the transcriptome of individual cells in organs and tissues. This approach has been used in single-cell studies of animal (Bakken *et al.*, 2018; Wu *et al.*, 2019) and plant (Neumann *et al.*, 2021) cells. Here, we describe its application to obtain insights into numerous bud cellular clusters, and targeted analysis of differentially expressed genes related to bud development.

Rhapsody and 10X are the most mainstream single-cell library-building platforms, and both provide excellent single-cell transcriptome library-building performance. The operation of 10X is simpler and more direct, and it can almost completely automate the database construction process, whereas Rhapsody has the potential for more flexible optimization of the number of nuclei captured and the library-building

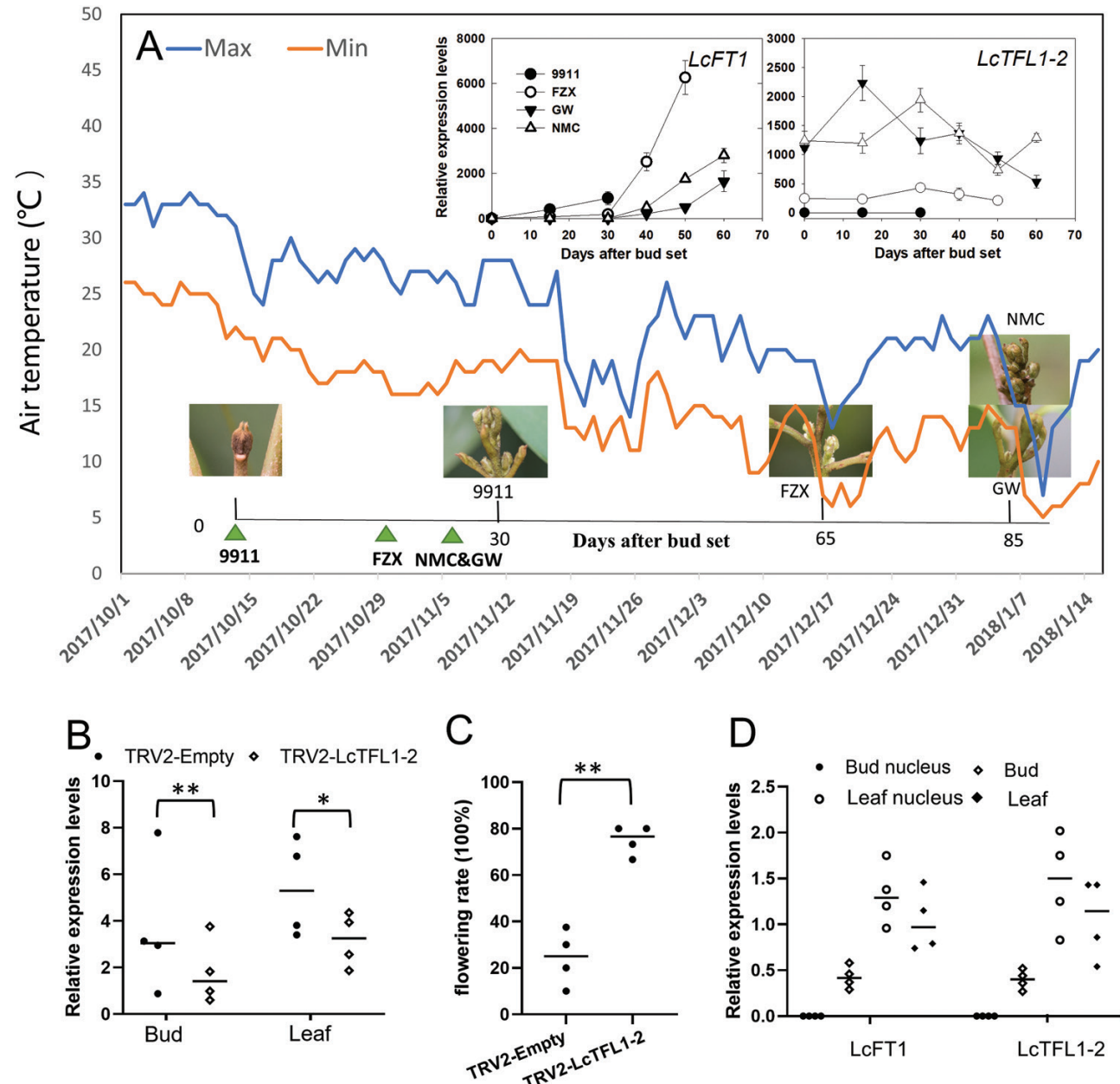


**Fig. 7.** Analysis of *LcFT1* and *LcTFL1-2* expression. (A) *LcFT1* and *LcTFL1-2* expression during floral induction and initiation in the leaf of litchi cultivars varies with flowering time. The green triangles indicate the bud set dates of the four cultivars tested [9911, Feizixiao (FZX), Nuomici (NMC), and Geivei (GW)]. The first photograph (left) shows a resting bud. The second photograph shows a floral bud of cv. 9911 observed at 30 d after bud set. The other photographs show floral buds of the other three cultivars observed at various days after bud set. (B) Expression of *Lc-TFL1-2* in response to virus-induced gene silencing (VIGS) in the bud and leaf of NMC based on PCR analysis. Each data point represents the expression level of a sample from an individual tree. (C) Significant increase in flowering rate in response to VIGS of *LcTFL1-2*. The flowering rate was calculated for each tree using 20 shoots (flowering rate=flowering shoot number/20  $\times$  100%) and each data point represents the flowering rate of that tree. (D) Absence of *LcFT1* and *LcTFL1-2* expression in the nucleus of litchi buds compared with leaf nucleus and intact bud and leaf samples. Asterisks indicate significant differences (\* $P<0.05$ , \*\* $P<0.01$ ; Student's *t*-test,  $n=4$ ).

process based on the pore-sedimentation principle, as well as a broader range of applications (Zhai and Xu, 2021). In this study, we selected the BD Rhapsody™ platform based on nuclear concentration and purity, the natural settling capture method used by the platform, which is less harmful to

nuclei, and cost performance. Owing to the complexity of plant tissues, the efficiency and quality of nuclear capture were critical for plant snRNA-seq. The number of captured cells was much higher with Rhapsody than with 10X at the same price. Additionally, using the Rhapsody platform,

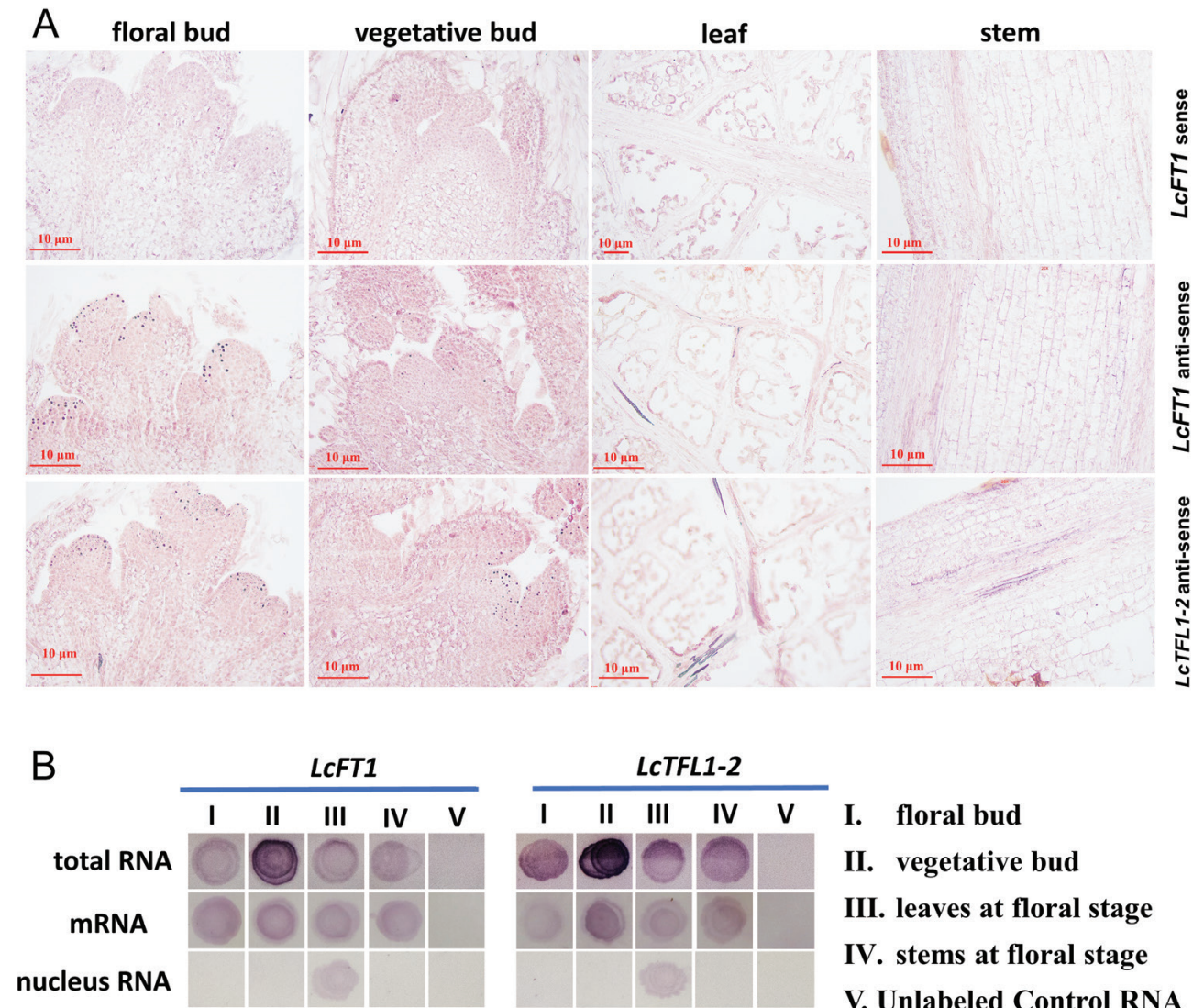


**Fig. 8.** *LcFT1* and *LcTFL1-2* expression in bud, leaf, and stem samples from litchi. (A) RNA *in situ* hybridization. Tissue sections were hybridized with either a *LcFT1* or a *LcTFL1-2* probe. There was no mRNA signal of *LcFT1* or *LcTFL1-2* in tissues hybridized with either *LcFT1* or *LcTFL1-2* sense RNA probe. The sense RNA probe of *LcFT1* is included as a reference. Scale bars=10 µm. (B) Dot-blot hybridization of total RNA, mRNA, and nuclear RNA extracted from different tissues of litchi with either a *LcFT1* or a *LcTFL1-2* probe.

large-volume and low-density nuclear suspensions can be used to reduce double-cell rates and thus increase the amount of effective data. Taking all these factors together, Rhapsody might be a better platform for plant snRNA-seq studies.

#### snRNA-seq profiles of the floral transition in litchi buds

Inconsistent flowering, especially for evergreen fruit crops such as litchi and longan (*Dimocarpus longan*), is a bottleneck in commercial production. Using the Solexa/Illumina sequencing platform, researchers have identified several transcripts involved in flowering in woody plants (Zhang *et al.*, 2014; Chen *et al.*, 2018; Wang *et al.*, 2019). However, the transition from vegetative to reproductive development occurs mainly in the

shoot apical meristem, and it is technically challenging to obtain meristem samples from apical buds. In the present study, we found that different bud types had distinctly different expression patterns, as is shown in the associated cell atlases, and that the F buds had both absent and unique cell populations compared with the other bud types (Fig. 2). Cell-type-specific reporters were used in a cell-sorting analytical pipeline to generate high-quality cell-type-specific transcriptomes of the litchi bud (Fig. 3). Mesophyll and epidermal cells accounted for the majority of cells (~60%) in the apical bud samples, while meristem cells accounted for only 5% (Supplementary Fig. S4). snRNA-seq analysis provided precise and comprehensive cell-type-specific gene expression data, which facilitated the discovery of gene and molecular regulatory networks.

In *A. thaliana*, it has been proposed that the vegetative state of the shoot apical meristem is under constant floral repression, which is broken only when the balance of the floral-promoting pathways outweighs the suppressive effects of the floral repressors (Yant et al., 2009). FD is an FT interactor, and the FT–FD complex directly promotes the expression of *SOC1*, *FUL*, and ultimately the floral meristem identity genes *AP1* and *LEAFY*, to trigger flowering (Yant et al., 2009). In this study, we investigated the expression patterns of flowering-time-related genes in FMCs of U, V, and F dominant cell clusters (Fig. 4G; Supplementary Fig. S6). We found that the putative litchi *SOC1* had much higher expression levels in FMCs of U and V buds than in FMCs of F buds. In *A. thaliana*, *FLC* and *SVP* function together in a repressor complex that integrates flowering induction signals to directly repress *SOC1* by binding to adjacent sites in its promoter (Li et al., 2008). Although the expression of both the putative litchi *FLC* and *SVP* floral repressors was much higher in the FMCs of U and V than F buds, a higher but not opposite expression pattern of *SOC1* was observed. This contrasting *SOC1* expression pattern in F cells might be explained by a negative relationship between *AP1* and *SOC1*. In *A. thaliana*, the repression of *SOC1* by *AP1* is necessary to prevent premature differentiation of the floral meristem, and thus floral reversion (Lee and Lee, 2010). In the woody perennial vine kiwifruit, functional and expression analyses suggested that *SOC1*-like genes may not have a role in the transition of flowering but may affect the duration of dormancy (Voogd et al., 2015). Similarly, lower expression of *SOC1* in F buds of woody litchi might be not associated with flower transition but with the growth potential of buds. The plant hormones gibberellins (GA) are known to influence the floral transition through the regulation of *SOC1* at the shoot apex (Wilson et al., 1992). In the current study, much higher expression of a putative *GAI*, a DELLA protein that represses the GA signaling pathway, was detected in FMCs of F buds than in V buds. This provides another possible explanation for the low expression of *SOC1* in F buds. Higher expression of *GAI* in FMCs of F buds might help to reduce the expression of *SOC1*, which thereby represses floral reversion and thus enhances flowering in fruit crops. In fruit crop production, paclobutrazole, a GA antagonist, is frequently applied to maintain bud rest and increase flowering rate.

Expression of the MADS-box gene *AP1* is generally considered to be a cardinal indicator of floral transition in buds. In this study, the expression of putative litchi *AP1* in the FMCs of F buds was much higher than in V and U buds (Fig. 4G). The expression of *AP1* showed a positive correlation with that of other flowering-time-related genes such as *FD*, *AGL8*, *AGL62*, and *SPL8* (Fig. 5). In *A. thaliana*, *LEAFY* is the first known meristem identity gene to be expressed after floral transition and it promotes floral meristem development (Ferrandiz et al., 2000). In our study, a positive correlation between the expression of putative *AGL142* and *LEAFY* suggests a process similar to that in *A. thaliana*, where an *AGL* gene functions upstream of *LEAFY*.

Considering these results, we propose a model for floral meristem identity events in litchi (Fig. 9). *LcFT1* (LITCHI002331) expression is initiated in leaves after prolonged chilling induction, is transported in the form of mRNA and protein to the shoot apex, and interacts with the bZIP transcription factor FD (LITCHI006416) there. The resulting FT–FD complex induces the expression of the floral integrators *AP1* (LITCHI005352) and *FUL* (AGL8, LITCHI023327) to activate the expression of floral meristem identity genes, such as *LEAFY* (LITCHI020239), and key regulators of flower morphogenesis, such as *AGL42* (LITCHI009244), *AGL62* (LITCHI008609), and *SPL8* (LITCHI025415), the latter of which affects female and male fertility in *A. thaliana* (Xing et al., 2013). We suggest that litchi *AP1* may repress the expression of the flowering integrator *SOC1* in the flower primordia to maintain a balance between indeterminant growth and differentiation.

#### *The critical role of LcTFL1-2 in floral transition and transport of LcFT1 and LcTFL1-2 mRNA*

Like *FT*, *TERMINAL FLOWER 1* (*TFL1*) encodes a small globular phosphatidylethanolamine-binding protein (PEBP) (Yoo et al., 2010), and in the litchi bud transcriptome, six putative members of the *PEBP* gene family were identified (Supplementary Fig. S6). Among them, *LcFT1* (LITCHI002331) was previously found to function as the main activator of litchi flowering (Ding et al., 2015). The florigen *FT* promotes the transition to reproductive development and flowering in a variety of plant species, whereas *TFL1* represses this transition (Wickland et al., 2015). Two putative *TFL1* genes (*LcTFL1-1* and *LcTFL1-2*) were detected in litchi (Supplementary Fig. S6); of these, the expression of *LcTFL1-2* was negatively related to flowering time, and VIGS further confirmed the role of *LcTFL1-2* in repressing flowering (Fig. 7A, B).

*TFL1* is likely to compete with *FT* for binding to *FD*, which could explain the opposite effects of *FT* and *TFL1* on flowering time (Hanano et al., 2011). In apple, down-regulation of *TFL1* accelerated flowering, while ectopic expression of kiwi-fruit *CEN*, a *TFL1* parologue, delayed flowering (Kotoda et al., 2006; Varkonyi-Gasic et al., 2013; Varkonyi-Gasic et al., 2019). In the present study, at floral initiation, the expression levels of *LcFT1* and *LcTFL1-2* in the leaves of the early-season cultivar 9911 was much lower than that in the three later-season cultivars (Fig. 7A). These results suggest that *LcTFL1-2* also serves as a deciding factor in the floral transition of litchi. To confirm the different roles of *LcFT1* and *LcTFL1-2* in litchi flowering, *in vivo* *LcFT1*VIGS assays using different litchi cultivars should be conducted in future research.

We did not detect the expression of any putative *FT* and *TFL1* genes based on snRNA-seq data (Supplementary Fig. S6). However, expression of *LcTFL1-2* and *LcFT1* was observed in litchi buds by qRT–PCR (Fig. 7B), and the non-nuclear expression of *LcFT1* and *LcTFL1-2* in litchi buds was

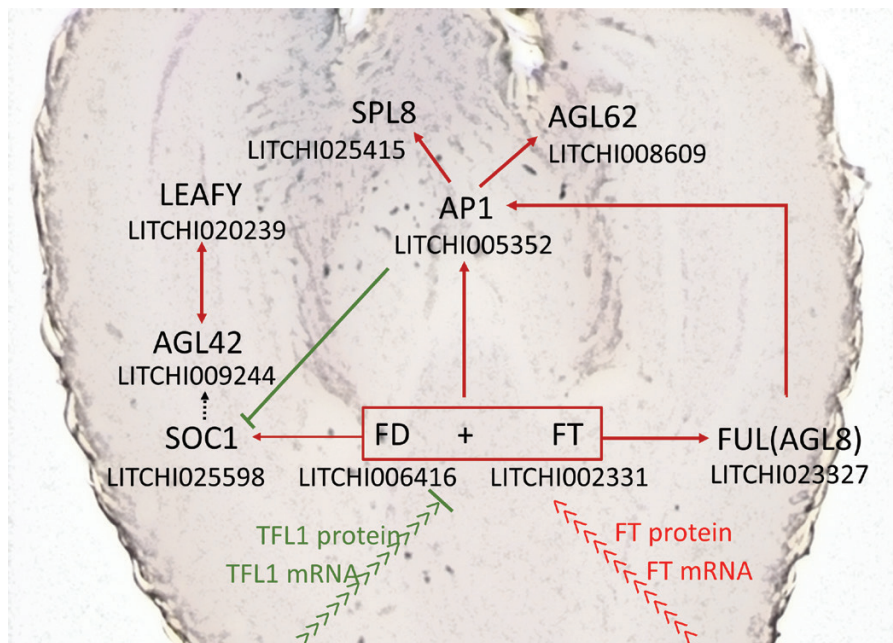


**Fig. 9.** Diagram of possible genetic interactions leading to flowering in litchi. The image in the background is a litchi bud. FT protein is directly transported from the leaf or translated from the transportable *FT* mRNA in the meristem, where it binds with FD to trigger the expression of the floral integrator genes *AP1* and *FUL*, which activate the expression of downstream flower morphogenesis genes such as *AGL62* and *SPL8*. The *FT*-FD-activated *SOC1* is negatively regulated by *AP1* to prevent premature floral differentiation and thus floral reversion. The binding of *FT* and FD might be influenced by *TFL1*, a mRNA transportable floral repressor. Up-regulation is represented by red arrows and repression is represented by green lines with bar ends.

also determined by comparing extracted bud nuclei and intact bud samples. The presence of leaf nuclei expressing *LcFT1* and *LcTFL1-2* mRNAs in the stem phloem cells and shoot apical meristems detected by *in situ* and dot-blot hybridization assays indicated that *LcFT1* and *LcTFL1* mRNA mobility may contribute to systemic florigen signaling in floral induction in litchi (Fig. 8).

The proteins encoded by *FT* in *A. thaliana* and their orthologs in other plant species are synthesized in leaf phloem companion cells in response to environmental cues and are transported to the shoot apical meristem through the phloem to provoke the initiation of floral meristems, and this long-distance trafficking is mediated by several regulators (Liu *et al.*, 2020). Modulation of *FT* transport affects plant flowering, and *FT* protein sequestration in cellular membranes through binding to the phospholipid phosphatidylglycerol is known to modulate temperature-responsive flowering (Susila *et al.*, 2021). Li *et al.* (2009) used novel RNA mobility assays to determine that *A. thaliana* *FT* mRNA, independent of the *FT* protein, moves systemically through the plant, but whether *FT* mRNA can move into the shoot apex is still unknown. Although plant meristems exclude exogenous RNA, a few cellular RNAs, such as the tomato *KNOTTED1-like homeobox* fusion transcript and the RNA of *GAI*, have been shown to move through the phloem and into the meristem in *A. thaliana* and tomato (Kim *et al.*, 2001; Haywood *et al.*, 2005). In this study, we detected both *LcFT1* and *LcTFL1-2*

mRNAs in the shoot apex (Fig. 7). In plant growth regulation, mRNA template translocation may be more efficient than protein transport. Moreover, long-distance movement of *A. thaliana* *FT* mRNA has been demonstrated to play a role in floral induction (Lu *et al.*, 2012). The discovery of *LcFT1* and *LcTFL1-2* mRNAs being transported from the leaf to the apical meristem sheds new light on the nature of mobile florigens in woody plants. The presence of comparable levels of *LcTFL1-2* and *LcFT1* mRNA in the floral bud but much less *LcFT1* than *LcTFL1-2* in the vegetative bud suggests that an increase in *LcFT1* expression is essential for floral transition in litchi; nevertheless, the transcription of *LcTFL1-2* may determine the amount of *LcFT1* required for successful floral initiation.

## Supplementary data

The following supplementary data are available at [JXB online](#).

Fig. S1. Protoplast isolation and high-purity nucleus separation and loading.

Fig. S2. Detailed workflow diagram summarizing high-purity nucleus separation, WTA library construction, sequencing, and data visualization.

Fig. S3. Quality control of sn-RNA sequencing data.

Fig. S4. Extended data from Figs 2, 3, and 5.

Fig. S5. Expression of flowering genes in the differentiation trajectories.

Fig. S6. Differential expression pattern of key flowering time genes.

Table S1. Primer sequences used for *LcTFL1-2* qRT-PCR expression and mRNA hybridization.

## Acknowledgements

The authors would like to thank Shuzhen Zhai, Becton Dickinson Medical Devices, for technical assistance, and Dr Minglei Zhao, Jietang Zhao, and Professor Jianguo Li for their valuable suggestions.

## Author contributions

HCW, MCY, and ZCW developed the concept; MCY, ZCW, and YSX developed the methodology; MCY, ZCW, and WSG performed the experiments; MCY, RYC, XMH, and GBH were responsible for data curation; HCW, FA, and MCY wrote the manuscript.

## Conflict of interest

The authors declare no competing interests.

## Funding

This work was supported by the Laboratory of Lingnan Modern Agriculture Project (NZ NT2021004), the Guangzhou Science and Technology Project (202103000057 and 202206010023), and the China Litchi and Longan Industry Technology Research System (project no. CARS-32-08).

## Data availability

The snRNA-seq data have been deposited in NCBI database (SRA: PRJNA909160).

All other data supporting the findings of this study are available within the paper and within its supplementary data published online.

## References

- Abe M, Katsumata H, Komeda Y, Takahashi T.** 2003. Regulation of shoot epidermal cell differentiation by a pair of homeodomain proteins in *Arabidopsis*. *Development* **130**, 635–643.
- André D, Marcon A, Lee KC, Goretti D, Zhang B, Delhomme N, Schmid M, Nilsson O.** 2022. *FLOWERING LOCUS T* paralogs control the annual growth cycle in *Populus* trees. *Current Biology* **32**, 2988–2996.e4.
- Andrés F, Coupland G.** 2012. The genetic basis of flowering responses to seasonal cues. *Nature Reviews Genetics* **13**, 627–639.
- Bakken TE, Hodge RD, Miller JA, et al.** 2018. Single-nucleus and single-cell transcriptomes compared in matched cortical cell types. *PLoS One* **13**, e0209648e209648.
- Bao S, Hua C, Shen L, Yu H.** 2020. New insights into gibberellin signaling in regulating flowering in *Arabidopsis*. *Journal of Integrative Plant Biology* **62**, 118–131.
- Belkina AC, Ciccolella CO, Anno R, Halpert R, Spidlen J, Snyder-Cappione JE.** 2019. Automated optimized parameters for T-distributed stochastic neighbor embedding improve visualization and analysis of large datasets. *Nature Communications* **10**, 5419.
- Benloch R, Berbel A, Serrano-Mislata A, Madueno F.** 2007. Floral initiation and inflorescence architecture: a comparative view. *Annals of Botany* **100**, 659–676.
- Buttner M, Singh KB.** 1997. *Arabidopsis thaliana* ethylene-responsive element binding protein (AtEBP), an ethylene-inducible, GCC box DNA-binding protein interacts with an ocs element binding protein. *Proceedings of the National Academy of Sciences of the United States of America* **94**, 5961–5966.
- Chen X, Qi S, Zhang D, Li Y, An N, Zhao C, Zhao J, Shah K, Han M, Xing L.** 2018. Comparative RNA-sequencing-based transcriptome profiling of buds from profusely flowering ‘Qinguan’ and weakly flowering ‘Nagafu no. 2’ apple varieties reveals novel insights into the regulatory mechanisms underlying floral induction. *BMC Plant Biology* **18**, 370.
- Ding F, Zhang S, Chen H, Su Z, Zhang R, Xiao Q, Li H.** 2015. Promoter difference of *LcFT1* is a leading cause of natural variation of flowering timing in different litchi cultivars (*Litchi chinensis* Sonn.). *Plant Science* **241**, 128–137.
- Dobin A, Davis CA, Schlesinger F, Drenkow J, Zaleski C, Jha S, Batut P, Chaisson M, Gingeras TR.** 2013. STAR: ultrafast universal RNA-seq aligner. *Bioinformatics* **29**, 15–21.
- Dorca-Fornell C, Gregis V, Grandi V, Coupland G, Colombo L, Kater MM.** 2011. The *Arabidopsis* SOC1-like genes *AGL42*, *AGL71* and *AGL72* promote flowering in the shoot apical and axillary meristems. *The Plant Journal* **67**, 1006–1017.
- Ferrandiz C, Gu Q, Martienssen R, Yanofsky MF.** 2000. Redundant regulation of meristem identity and plant architecture by *FRUITFULL*, *APETALA1* and *CAULIFLOWER*. *Development* **127**, 725–734.
- Green MR, Sambrook J.** 2022. Dot and slot hybridization of purified RNA. *Cold Spring Harbor Protocols* **2022**. doi: [10.1101/pdb.prot101808](https://doi.org/10.1101/pdb.prot101808).
- Haghverdi L, Lun ATL, Morgan MD, Marioni JC.** 2018. Batch effects in single-cell RNA-sequencing data are corrected by matching mutual nearest neighbors. *Nature Biotechnology* **36**, 421–427.
- Hanano S, Goto K.** 2011. *Arabidopsis TERMINAL FLOWER1* is involved in the regulation of flowering time and inflorescence development through transcriptional repression. *The Plant Cell* **23**, 3172–3184.
- Haywood V, Yu TS, Huang NC, Lucas WJ.** 2005. Phloem long-distance trafficking of *GIBBERELLIC ACID-SENSITIVE* RNA regulates leaf development. *The Plant Journal* **42**, 49–68.
- Hicks KA, Albertson TM, Wagner DR.** 2001. *EARLY FLOWERING3* encodes a novel protein that regulates circadian clock function and flowering in *Arabidopsis*. *The Plant Cell* **13**, 1281–1292.
- Hsu CY, Adams JP, Kim H, et al.** 2011. *FLOWERING LOCUS T* duplication coordinates reproductive and vegetative growth in perennial poplar. *Proceedings of the National Academy of Sciences of the United States of America* **108**, 10756–10761.
- Hu G, Feng J, Xiang X, et al.** 2022. Two divergent haplotypes from a highly heterozygous lychee genome suggest independent domestication events for early and late-maturing cultivars. *Nature Genetics* **54**, 73–83.
- Jensen AB, Raventos D, Mundy J.** 2002. Fusion genetic analysis of jasmonate-signalling mutants in *Arabidopsis*. *The Plant Journal* **29**, 595–606.
- Kim M, Canio W, Kessler S, Sinha N.** 2001. Developmental changes due to long-distance movement of a homeobox fusion transcript in tomato. *Science* **293**, 287–289.
- Kotoda N, Iwanami H, Takahashi S, Abe K.** 2006. Antisense expression of *MdTFL1*, a *TFL1*-like gene, reduces the juvenile phase in apple. *Journal of the American Society for Horticultural Science* **131**, 74–81.
- Lai B, Hu B, Qin YH, Zhao JT, Wang HC, Hu GB.** 2015. Transcriptomic analysis of *Litchi chinensis* pericarp during maturation with a focus on chlorophyll degradation and flavonoid biosynthesis. *BMC Genomics* **16**, 225.
- Lazar A, Valverde F, Pineiro M, Jarillo JA.** 2012. The *Arabidopsis* E3 ubiquitin ligase HOS1 negatively regulates CONSTANS abundance in the photoperiodic control of flowering. *The Plant Cell* **24**, 982–999.

- Lee J, Lee I.** 2010. Regulation and function of SOC1, a flowering pathway integrator. *Journal of Experimental Botany* **61**, 2247–2254.
- Lee JH, Kim JJ, Kim SH, Cho HJ, Kim J, Ahn JH.** 2012. The E3 ubiquitin ligase HOS1 regulates low ambient temperature-responsive flowering in *Arabidopsis thaliana*. *Plant and Cell Physiology* **53**, 1802–1814.
- Lee C, Kin SJ, Jin S, Susila H, Youn G, Nasim Z, Alavilli H, Chung KS, Yoo SJ, Ahn JH.** 2019. Genetic interactions reveal the antagonistic roles of *FT/TSF* and *TFL1* in the determination of inflorescence meristem identity in *Arabidopsis*. *The Plant Journal* **99**, 452–464.
- Li D, Liu C, Shen L, Wu Y, Chen H, Robertson M, Hellwell CA, Ito T, Meyerowitz E, Yu H.** 2008. A repressor complex governs the integration of flowering signals in *Arabidopsis*. *Developmental Cell* **15**, 110–120.
- Li C, Zhang K, Zeng X, Jackson S, Zhou Y, Hong Y.** 2009. A *cis* element within *Flowering Locus T* mRNA determines its mobility and facilitates trafficking of heterologous viral RNA. *Journal of Virology* **83**, 3540–3548.
- Liu L, Zhang Y, Yu H.** 2020. Florigen trafficking integrates photoperiod and temperature signals in *Arabidopsis*. *Journal of Integrative Plant Biology* **62**, 1385–1398.
- Lopez-Anido CB, Vatén A, Smoot NK, Sharma N, Guo V, Gong Y, Anleu Gil MX, Weimer AK, Bergmann DC.** 2021. Single-cell resolution of lineage trajectories in the *Arabidopsis* stomatal lineage and developing leaf. *Developmental Cell* **56**, 1043–1055.e4.
- Lou S, Chen S, Zhao X, Chen L, Zhang J, Fu H, Liu YG, Chen Y.** 2017. The far-upstream regulatory region of *RFL* is required for its precise spatial-temporal expression for floral development in rice. *Plant Molecular Biology* **93**, 185–195.
- Lu K, Huang N, Liu Y, Lu C, Yu T.** 2012. Long-distance movement of *Arabidopsis FLOWERING LOCUS T* RNA participates in systemic floral regulation. *RNA Biology* **9**, 653–662.
- Menzel CM, Waite GK.** 2005. Litchi and longan: botany, production, and uses. Wallingford: CABI Publishing.
- Meyerowitz EM, Bowman JL, Brockman LL, Drews GN, Jack T, Sieburth LE, Weigel D.** 1991. A genetic and molecular model for flower development in *Arabidopsis thaliana*. *Development* **1**, 157–167.
- Neumann M, Xu X, Smaczniak C, et al.** 2021. A 3D gene expression atlas of the floral meristem based on spatial reconstruction of single nucleus RNA sequencing data. *Nature Communications* **13**, 2838.
- Pichersky E, Bernatzky R, Tanksley SD, Cashmore AR.** 1986. Evidence for selection as a mechanism in the concerted evolution of *Lycopersicon esculentum* (tomato) genes encoding the small subunit of ribulose-1,5-bisphosphate carboxylase/oxygenase. *Proceedings of the National Academy of Sciences of the United States of America* **83**, 3880–3884.
- Putterill J, Varkonyi-Gasic E.** 2016. FT and florigen long-distance flowering control in plants. *Current Opinion in Plant Biology* **33**, 77–82.
- Rubio-Somoza I, Weigel D.** 2013. Coordination of flower maturation by a regulatory circuit of three microRNAs. *PLoS Genetics* **9**, e1003374.
- Sunaga-Franze DY, Muino JM, Braeuning C, et al.** 2021. Single-nucleus RNA sequencing of plant tissues using a nanowell-based system. *The Plant Journal* **108**, 859–869.
- Susila H, Juric S, Liu L, et al.** 2021. Florigen sequestration in cellular membranes modulates temperature-responsive flowering. *Plant Science* **373**, 1137–1142.
- Thomas H, Thomas HM, Ougham H.** 2000. Annuality, perenniability and cell death. *Journal of Experimental Botany* **51**, 1781–1788.
- Trapnell C, Cacchiarelli D, Grimsby J, Pokharel P, Li S, Morse M, Lennon NJ, Livak KJ, Mikkelsen TS, Rinn JL.** 2014. The dynamics and regulators of cell fate decisions are revealed by pseudotemporal ordering of single cells. *Nature Biotechnology* **32**, 381–386.
- Turck F, Fornara F, Coupland G.** 2008. Regulation and identity of florigen: *FLOWERING LOCUS T* moves center stage. *Annual Review of Plant Biology* **59**, 573–594.
- Turnbull C.** 2011. Long-distance regulation of flowering time. *Journal of Experimental Botany* **62**, 4399–4413.
- Tylewicz S, Tsuji H, Miskolczi P, Petterle A, Azeez A, Jonsson K, Shimamoto K, Bhalerao RP.** 2015. Dual role of tree florigen activation complex component *FD* in photoperiodic growth control and adaptive response pathways. *Proceedings of the National Academy of Sciences of the United States of America* **112**, 3140–3145.
- Varkonyi-Gasic E, Moss SMA, Voogd C, Wang T, Putterill J, Hellens RP.** 2013. Homologs of *FT*, *CEN* and *FD* respond to developmental and environmental signals affecting growth and flowering in the perennial vine kiwifruit. *New Phytologist* **198**, 732–746.
- Varkonyi-Gasic E, Wang T, Voogd C, Jeon S, Drummond RSM Gleave AP, Allan AC.** 2019. Mutagenesis of kiwifruit *CENTRORADIALIS*-like genes transforms a climbing woody perennial with long juvenility and axillary flowering into a compact plant with rapid terminal flowering. *Plant Biotechnology Journal* **17**, 869–880.
- Voogd C, Wang T, Varkonyi-Gasic E.** 2015. Functional and expression analyses of kiwifruit SOC1-like genes suggest that they may not have a role in the transition to flowering but may affect the duration of dormancy. *Journal of Experimental Botany* **66**, 4699–4710.
- Wang S, Gao J, Xue J, Xue Y, Li D, Guan Y, Zhang X.** 2019. De novo sequencing of tree peony (*Paeonia suffruticosa*) transcriptome to identify critical genes involved in flowering and floral organ development. *BMC Genomics* **20**, 572.
- Wickland D, Hanzawa Y.** 2015. The *FLOWERING LOCUS T/TERMINAL FLOWER 1* gene family: functional evolution and molecular mechanisms. *Molecular Plant* **8**, 983–997.
- Wigge PA, Kim MC, Jaeger KE, Busch W, Schmid M, Lohmann JU, Weigel D.** 2005. Integration of spatial and temporal information during floral induction in *Arabidopsis*. *Science* **309**, 1056–1059.
- Wilson RN, Heckman JW, Somerville CR.** 1992. Gibberellin is required for flowering in *Arabidopsis thaliana* under short days. *Plant Physiology* **100**, 403–408.
- Wu ZC, Zhang JQ, Zhao JT, Li JG, Huang XM, Wang HC.** 2018. Biosynthesis of quebrachitol, a transportable photosynthate, in *Litchi chinensis*. *Journal of Experimental Botany* **69**, 1649–1661.
- Wu H, Kirita Y, Donnelly EL, Humphreys BD.** 2019. Advantages of single-nucleus over single-cell RNA sequencing of adult kidney: rare cell types and novel cell states revealed in fibrosis. *Journal of the American Society of Nephrology* **30**, 23–32.
- Xing S, Salinas M, Garcia-Molina A, Hohmann S, Berndtgen R, Huijser P.** 2013. *SPL8* and miR156-targeted *SPL* genes redundantly regulate *Arabidopsis* gynoecium differential patterning. *The Plant Journal* **75**, 566–577.
- Yang MC, Wu ZC, Huang LL, Abbas F, Wang HC.** 2022. Systematic methods for isolating high purity nuclei from ten important plants for omics interrogation. *Cells* **11**, 3919.
- Yant L, Mathieu J, Schmid M.** 2009. Just say no: floral repressors help *Arabidopsis* bide the time. *Current Opinion in Plant Biology* **12**, 580–586.
- Yoo SJ, Chung KS, Jung SH, Yoo SY, Lee JS, Ahn JH.** 2010. *BROTHER OF FT AND TFL1 (BFT)* has *TFL1*-like activity and functions redundantly with *TFL1* in inflorescence meristem development in *Arabidopsis*. *The Plant Journal* **63**, 241–253.
- Zhai N, Xu L.** 2021. Pluripotency acquisition in the middle cell layer of callus is required for organ regeneration. *Nature Plants* **7**, 1453–1460.
- Zhang H, Wei Y, Shen J, Lai B, Huang X, Ding F, Su Z, Chen H.** 2014. Transcriptomic analysis of floral initiation in litchi (*Litchi chinensis* Sonn.) based on de novo RNA sequencing. *Plant Cell Reports* **33**, 1723–1735.
- Zhang T, Xu Z, Shang G, Wang J.** 2019. A single-cell RNA sequencing profiles the developmental landscape of *Arabidopsis* root. *Molecular Plant* **12**, 648–660.
- Zhang T, Chen Y, Liu Y, Lin W, Wang J.** 2021a. Single-cell transcriptome atlas and chromatin accessibility landscape reveal differentiation trajectories in the rice root. *Nature Communications* **12**, 2053.
- Zhang T, Chen Y, Wang J.** 2021b. A single-cell analysis of the *Arabidopsis* vegetative shoot apex. *Developmental Cell* **56**, 1056–1074.e8.
- Zhu Y, Klasfeld S, Jeong CW, Jin R, Goto K, Yamaguchi N, Wagner D.** 2020. TERMINAL FLOWER 1-FD complex target genes and competition with *FLOWERING LOCUS T*. *Nature Communications* **11**, 5118.